Combustion of Agricultural Wastes/Coal in Circulating Fluidized Bed

Mahmoud A M Youssef, Hamada M Abdelmotalib

Abstract*: *This paper presents an experimental investigation on circulating fluidized bed (CFB) combustion of one of agricultural wastes (faba bean hulls) and co-combustion faba bean hulls and Egyptian (Sinai) coal. The test rig is a pilot scale CFB combustor of 145 mm inner diameter, 2 m tall and 100 kW thermal capacity. The influences of excess air, degree of air staging, bean hull particle size and coal share were studied. Temperature, heat flux, CO, NOx and SO_2 concentrations along the reactor height and flue gas out from cyclone were measured. The combustion efficiency was calculated based on CO emission and unburned char in flue gas. The results showed that size reduction of bean hulls results in lower CO and NOx emissions. The induction of secondary air has a negative effect on combustion efficiency. The highest efficiency recorded for bean hulls combustion was 98.5% at excess air ratio (EA) =1.09 without secondary air. Co-combustion of Sinai coal and bean hulls reduced CO and NOx emissions but increased SO2 emissions. The results suggest that bean hulls are potential fuel that can be utilized for efficient and clean energy production by using CFB combustion system especially at co-combustion.

Keywords: fluidized bed, combustion, agricultural wastes, coal, emission, efficiency

I. INTRODUCTION

Biomass is one of the most important resources of renewable energy. With the depletion of oil sources and concerns about global warming, the use of biomass is being considered more frequently [1]. Many researches demonstrate the promise of using agricultural wastes as alternative biofuel such as rice husk [2], rice straw [3], cotton stalks [4], pine chips [5], and olive husk [6], [7].

In Egypt, most electrical energy is generated from thermal power plants. The majority of these plants operate with natural gas, which will be depleted in little decades. With a scope on the future, Egypt needs a gradual resolution to fossil fuels with renewable energy such biomass fuels. Biomass includes a large variety types with different combustion characteristics [8].

Among the proven combustion technologies (such as fluidized bed, suspension-firing and grate firing), the fluidized bed technology, is reported to be the most efficient and suitable for the energy utilization of agricultural and wood residues. For example, an efficient and sustainable combustion of a conical fluidized bed system was performed using sawdust, rice husk and pre-dried bagasse in wide ranges of excess air and combustor load [9].

Rice husk is difficult to be fluidized and adding silicon sand and coal improves the fluidization during experiments on a cold model [2]. However, for proper fluidization, inert bed material should be used to facilitate biomass fluidization. Alumina bed can mix well in cotton stalk experiments [4].

Generally, most biomass fuels cannot easily fluidize due to irregular particle shapes [10] or high moisture/ash content [11]. Another problem of fluidized bed combustion of biomass is the agglomeration phenomenon. The occurrence of this phenomenon during fluidized bed processing of biomass fuels was investigated in [6]. The phenomenon was attributed to the alkali content in biomass materials that gives rise to low melting compounds in combination with SiO_2, normally present in bed materials. Combustion of refuse-derived fuel alone or together with other biomass leads to super-heater fouling and corrosion due to vaporization and condensation of alkali chlorides. The portion of refused-derived fuel up to 40% was used without risk to boilers [12].

The co-firing coal and biomass in CFB confirmed that the increase in biomass share resulted in an increase of CO concentration in the flue gas [13]. For more contribution of biomass to the commercial energy demand, the technical enhancements should focus on improving environmental impacts and combustion efficiency. In the fluidized bed systems, the major harmful pollutants emitted from biomass combustion are the emissions of CO, NO_x and SO_2 [4]. As a case study, rice husk combustion shows that the air split and gas velocity have great effect on the emissions and combustion efficiency [2].

With respect to the environmental limits, the combustion of biomass in CFB is preferable than SFB for various biomass fuels [8]. The combustion of some main biomass fuels in Egypt was investigated and showed high combustion efficiency in CFB [14, 15]. Hence, combustion studies of more Egyptian biomass fuels must be continued largely and deeply.

In the present study, the tested biomass fuel is faba-bean seed coats (bean hulls) which are produced as a waste from the first leguminous crop in Egypt. Co-combustion of bean hulls and Egyptian (Sinai) coal was investigated. The experiments were carried out on a 100 kW-CFB pilot scale located in the heat laboratory, Faculty of Engineering, Minia University.

Revised Manuscript Received on April 17, 2020.
***** Correspondence Author
Mahmoud A M Youssef *, Department of Mechanical Engineering, Jouf University, Saudi Arabia Kingdom
Mechanical Power Engineering Department, Minia University, Egypt
Email: myou_1@yahoo.com
Hamada M Abdelmotalib, Mechanical Power Engineering Department, Minia University, Egypt

The study focused on the effects of staged air and excess air ratio (EA) on the temperature and heat flux profiles and the combustion efficiency in the CFBC, as well as on the major emissions (CO, NO_x and SO_2).

II. EXPERIMENTAL

A. Experimental facilities

The CFB test rig includes reactor and the systems of bed recirculation, fuel feeding, air supply, and exhaust gas. Figure 1 shows an overall schematic of the CFB test rig. The reactor is an insulated steel cylinder with 145 mm inner diameter, 2 m height, and 12 mm wall thickness. Secondary air is admitted via two inlets on the reactor at heights of 0.3 m and 0.7 m above the distributor plate. The bed recirculation system includes connecting pass (connects between the reactor and the cyclone), cyclone, and return leg. The circulating solids are returned to the reactor at 200 mm above the air distributor through the return leg which is inclined with 45o. During the feeding of the solid fuel through this leg, it mixes with the returned solids. Air is used as a career for the fuel and returned solids to the reactor with the aid of gravity. The main air supply is a blower of 15 kW capacity and 2850 rpm. The primary air is admitted to the distributor through a cone vessel of 100 mm bottom diameter and 140 mm top diameter. The primary air is preheated by using an electric heater of 4.8 kW capacity. The distributor has 35 nozzles. Each nozzle is of 10 mm outer diameter, 5 mm inner diameter and has four holes of 2.5 mm diameter on the circumstance. The feeding mechanism of solid fuels is a screw feeder is derived by a low speed motor. A gaseous fuel (supplied from four gas bottles) is premixed with the primary air before entering the reactor. A suction fan is used to suck the flue gases to the chimney.

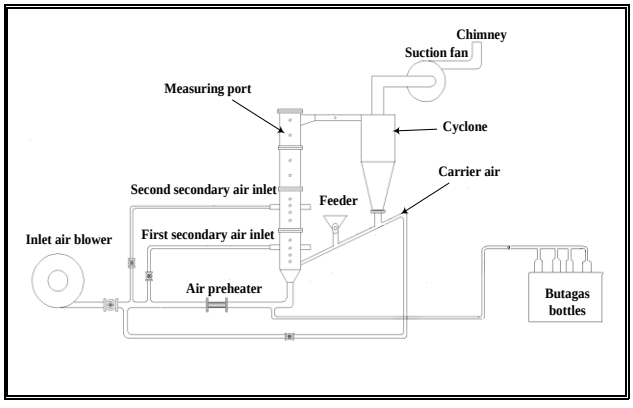

Figure 1: Schematic diagram of circulating fluidized bed.

The temperatures along the reactor were measured by a shielded thermocouple type K. The flue gas analysis is carried out along the reactor and before exiting from the chimney. The concentration of O_2, CO, CO_2, SO_2 and NO_x were measured by an electrochemical cells analyzer. Then, the measured emissions of CO, NO_x and SO_2 were recalculated based on 7% O_2 by volume in the flue gas. The accuracy of gas measurement was ± 4%. A plug-type heat flux meter is used to measure the heat flux to the reactor walls.

There are two copper constantan thermocouples inside the plug, separated by known distance along the axis of the plug. Hence, the heat flux to the reactor wall can be estimated at every measuring port in kW/m^2. The flow rate of air and gaseous fuel are measured by calibrated orifices. The solid fuel is fed to the furnace at selected (pre-set.) feed rates by the screw conveyor mechanism. Samples of fly ash in flue gas were collected after the suction fan and were analyzed for combustibles.

B. Fuel characteristics and bed material

The bed material is silica sand of 0.543 mm mean particle diameter and 1414 kg/m^3 bulk density. The faba-bean hull has an irregular boat-like shape and its dimensions are around 10 mm length, 5 mm width and 3 mm depth as shown in Fig. 2. The crushed bean hull is less than 3 mm in length.

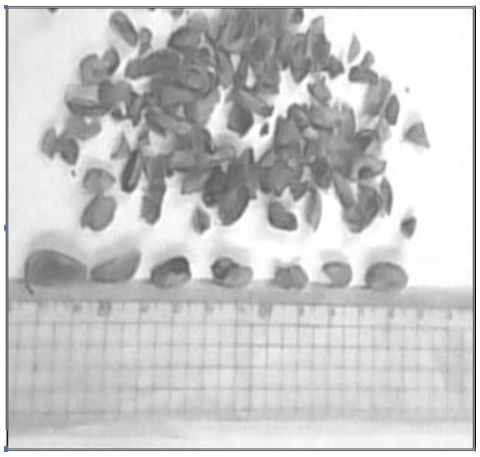

a- Before crushing.

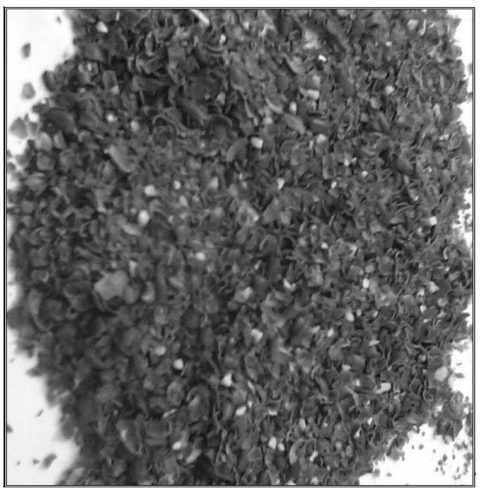

b- After crushing.

Figure 2: Photo of faba bean hulls.

The proximate and ultimate analysis and other properties of bean hulls and Sinai coal are given in Table 1. A commercial gaseous fuel (butagas) is used to start up the combustion process. Butagas is a mixture of 70% butane and 30% propane by volume.

Table 1: The properties of faba bean hulls and Sinai coal

	Faba-bean hulls	Sinai coal [15]
Ultimate analysis:		
H_2O %	10.6	3.8
ash %	10.5	9.8
C %	17.04	67.3
H %	6	5.54
N %	2.12	0.99
O %	53.74	10.26
S %	0.0	2.22
Proximate analysis		
volatiles %	62	48.9
fixed carbon %	17	37.5
H_2O %	10.5	3.8
ash %	10.5	9.8
A : F[1]	1.68	9.37
Bulk density kg/m^3	300	690
Real density kg/m^3	650	1600
LHV[2] kJ/kg	12830	27976
Mean particle size mm	1.07 (crushed)	0.9

[1] Stoichiometric air to fuel ratio [2] lower heating value.

C. Operating conditions

The bed is heated prior to admitting solid fuel by burning a butagas/air mixture. Solid fuel is fed by the screw feeder. The butagas supply is gradually decreased and stopped completely after the combustion is self-sustained. The electric heater is turned on during the start up procedure and stays on until the combustion process of solid fuel stabilizes then turned off.

Experiments focused on the effect of staged air, excess air ratio, size of bean hulls and coal share on the combustion characteristics such as temperature, heat flux and gas emission. Experiments can be divided into two groups. The first group deals with the combustion of bean hulls (before crushing and after crushing). The second group deals with the co-combustion of bean hulls and Sinai coal. The temperature, heat flux and gas emissions were measured along the reactor. The gas emissions were also measured before exit from chimney. All operating parameters of bean hulls combustion are shown in Table 2, and of co-combustion with Sinai coal in Table 3.

Table 2: General layout of the experimental proceeds of faba bean hulls combustion.

Fuel	Faba bean hulls (before crushing)					Faba bean hulls (after crushing)			
Experiment No.	1	2	3	4	5	1	2	3	4
Primary air flow rate, kg/h	72	106	96	85	64	85	90	93	98
Fuel feed rate, kg/h	30					30			
Excess air ratio (EA)	1.22	1.8	1.63	1.44	1.09	1.1	1.2	1.3	1.4
Secondary air ratio (SAR) %	0-20-40-50					0			
Mass of bed, kg	3					3			
Temperature of primary air, °C	110					110			
Thermal load, kW	107					107			

Table 3: General layout of the experiments of co-combustion of bean hulls and Sinai coal.

Fuel	bean hulls and Sinai coal mixture			
Experiment No.	1	2	3	4
Coal share% (thermal)	25	50	75	100
Coal feed rate, kg/h	3	6	9	12
Primary air flow rate, kg/h	170	190	185	190
Bean hulls feed rate, kg/h	21	14	7	0
Excess air ratio (EA)	1.09	1.2	1.4	1.7
Secondary air ratio (SAR) %	50			
Mass of bed, kg	3			
Temperature of primary air, °C	110			
Thermal load, kW	100			

The gas emissions were measured after the cyclone and related to 7% O_2 in flue gas. Based on CO emission and unburned carbon content in fly ash, the combustion efficiency can be calculated for biomass fuels and Sinai coal. The unburned carbon content in fly ash (at chimney) was analyzed and found to be in the range of 0.875– 3.9 % (by weight). Combustion efficiency (η_c) is mathematically determined from equations (1, 2 and 3).

$$\eta_{c} = \frac{Q_{in} - Q_{co} - Q_{un}}{Q_{in}} \quad (1)$$

$$Q_{co} = m_{co} * (C.V)_{CO} \quad (2)$$

$$Q_{un} = m_{ash} * char\% * \frac{1}{1 - char} * (C.V)_{carbon} \quad (3)$$

where:

Q_{in} The heat input.

Q_{co} The heat losses due to incomplete combustion of carbon.

$C.V_{CO}$ The calorific value of carbon monoxide = 10,160 kJ/kg.

Q_{un} The heat loss due to unburned carbon in fly ash.

$C.V_{carbon}$ The calorific value of carbon = 33,829 kJ/kg.

III. RESULTS AND DISCUSSION

A. Bean hulls combustion

A.1 Temperature distribution

Figure 3 shows the temperature distribution along the CFB reactor at different values of excess air ratio (EA). It is obvious that the temperature exhibits nearly one trend. The temperature decreases gradually along the reactor due to heat losses through chamber walls (despite the insulation). The highest temperatures were at the reactor bottom at 0.1 m height above the distributor. As expected, temperature values decrease with increasing EA (figures 3 a, b, c, d). The highest temperature was in the range between 900°C and 1000°C. Studying the influence of varying secondary air ratio SAR (the ratio of secondary air to total combustion air) indicates that the SAR of 0% offers higher temperature levels than the other SARs.

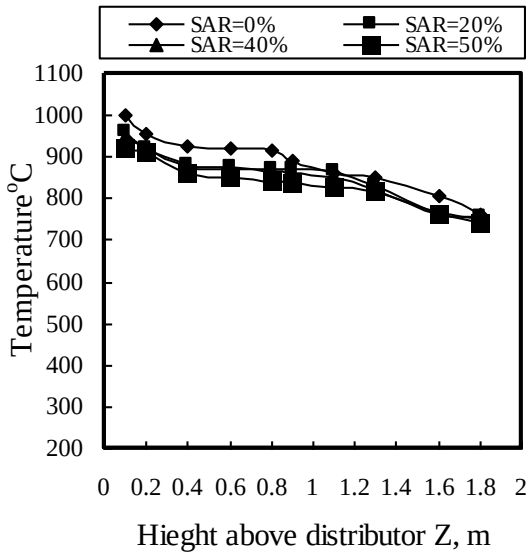

(a)

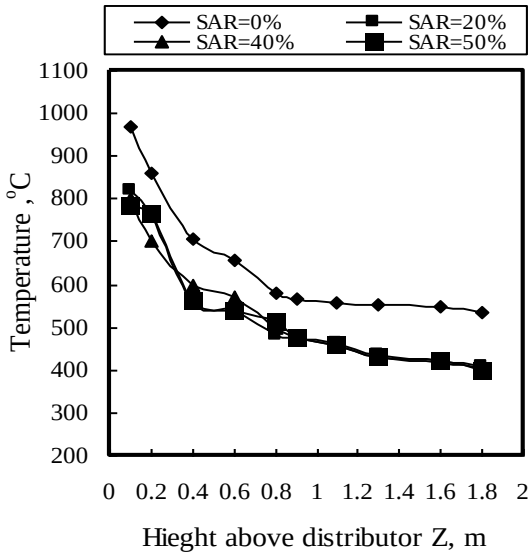

(b)

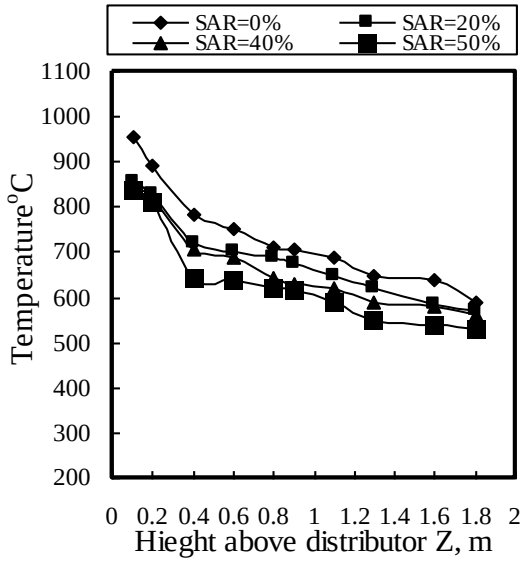

(c)

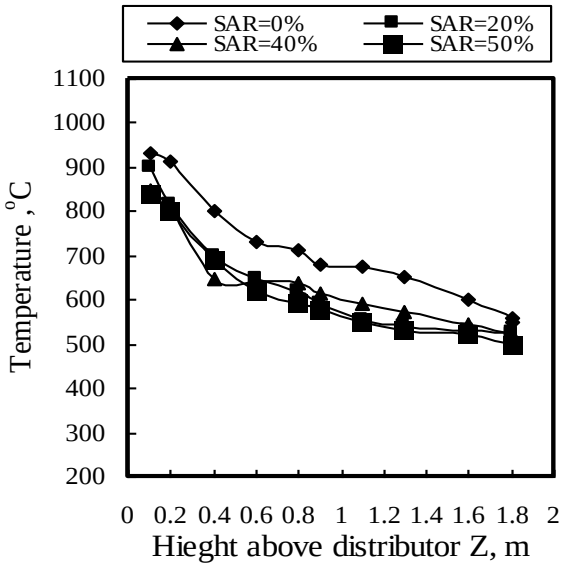

(d)

Figure 3: Temperature distribution along the reactor for bean hulls combustion.

The temperature distribution for the crushed bean hulls at EA =1.4 and SAR=0% is shown in Figure 4. It can be noticed that the reduction in hull size (from d_m= 5 mm to 1.07 mm) raises the temperature levels along the reactor relatively but has no great effect on temperature distribution.

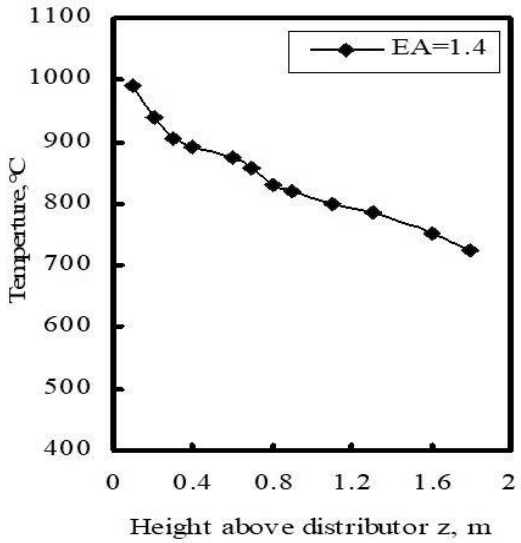

Figure 4: Temperature distribution along the reactor for crushed bean hulls combustion

A.2 Heat flux

Figure 5 shows the heat flux at various heights of the reactor. Comparing the temperature and heat flux figures clarifies that the heat flux has a similar trend to the temperature distribution along the reactor. The heat flux decreases gradually along the reactor due to heat losses through walls and the admission of secondary air. Maximum heat flux is about 90 kW/m^2 at height of 0.1 m above the distributor at SAR=0% and EA values of 1.09 and 1.22.

The values of heat flux are varied between about 20 kW/m^2 and 90 kW/m^2.

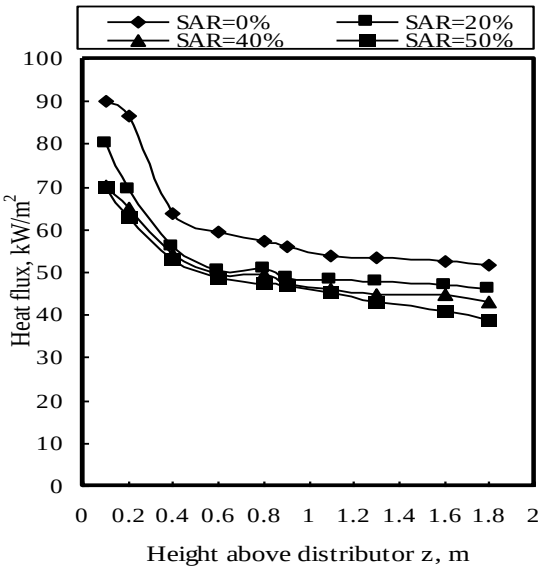

(a)

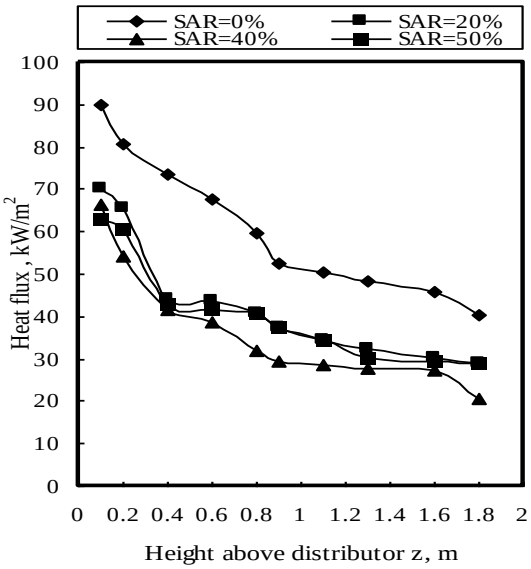

(b)

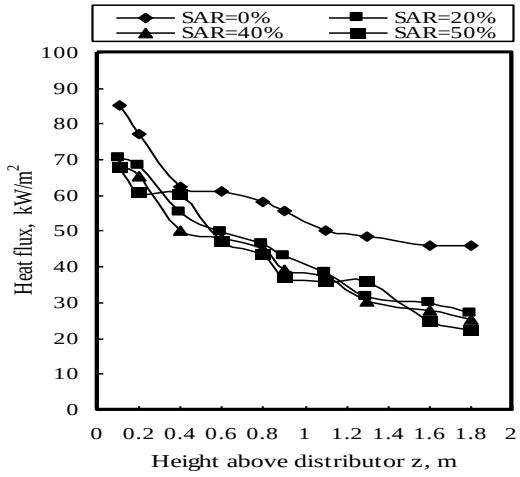

(c)

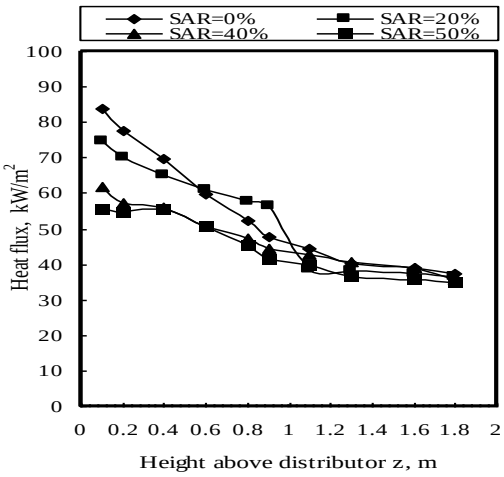

(d)

Figure 5: Heat flux along the reactor for bean hulls combustion.

Figures (6) shows the heat flux for the crushed bean hulls at EA =1.4. It is noticed that, the reduction in fuel size has no clear effect on heat flux, as clarified previously for the temperature.

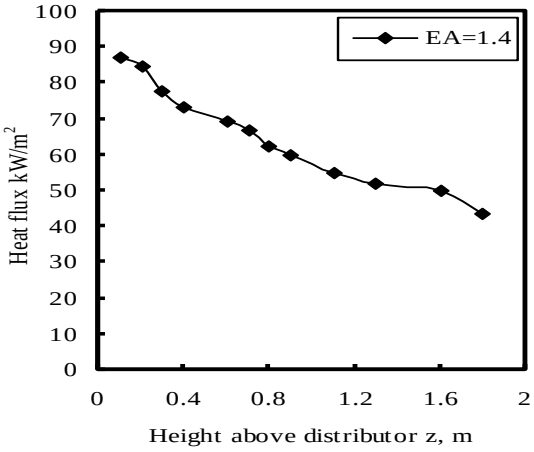

Figure 6: Heat flux along the reactor for crushed bean hulls combustion

A.3 Gas emissions

The influence of EA variation on the CO emissions is shown in figure 7a. It can be seen that CO emissions increase with increasing EA. This may be due to the cooling effect and decreasing in bed temperature caused by excess air. Figure 7b shows the CO emission at various values of SAR and EA= 1.09 (where the lowest values of CO emissions exist). It is noticed that increasing SAR to 50%, increases the CO emissions from 0.38% to 0.58% with an increase about 60%. The relatively high values of CO emission can be explained in light of the cooling effect of secondary air admission in addition to the relatively large size of bean hulls particle (d=5mm) and its irregular shape.

In order to reduce the CO emission, additional combustion experiments were carried out using crushed bean hulls. Preliminary experiments on the crushed bean hulls showed that the secondary air admission always increases the CO emissions. Therefore, the experiments carried out without secondary air, only were presented. These experiments were carried out with different values of EA as shown in Fig. 8a. The CO emission decreases with EA increase and it reaches a minimum value of 0.215% at EA =1.4. It is clear that the excess air, here, plays a positive role in completing the combustion process. CO emission distribution, without relating to 7% O_2 in flue gas, along the CFB reactor at EA =1.4 is shown in figure 8b. It can be observed that the CO emissions increase with increasing the height above the distributor till z=0.8 m and then asymptote to almost a constant value of 0.1%.

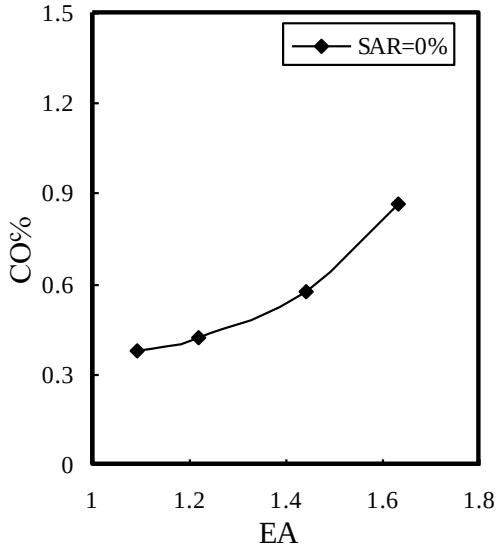

(a)

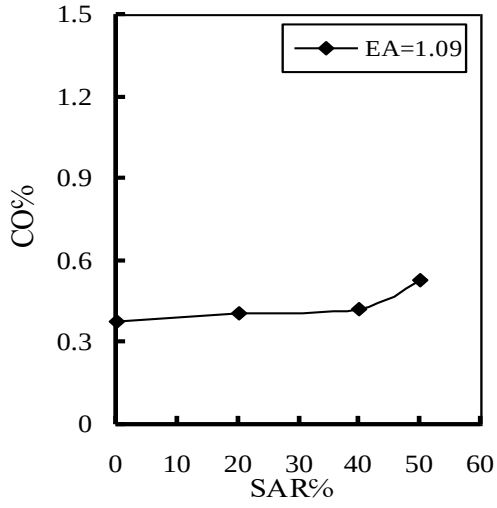

(b)

Figure 7: CO emissions for bean hulls combustion: (a) at different EA. (b) at different SARs.

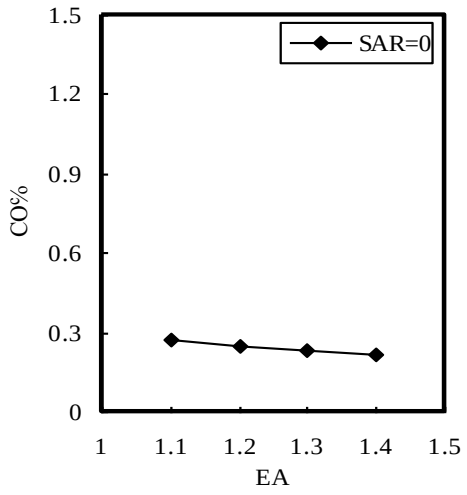

(a)

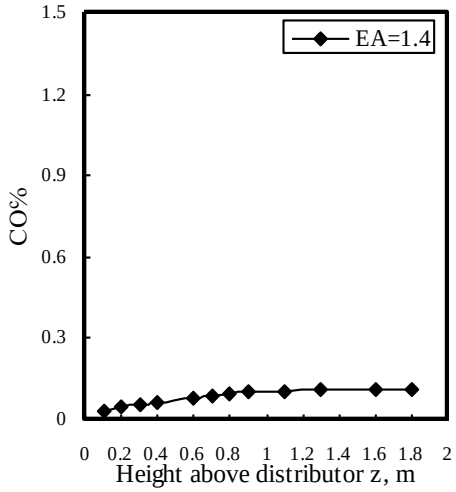

(b)

Figure 8: CO emissions for crushed bean hulls (a) at different EA. (b) along the reactor.

Figure 9a shows the NOx emissions of bean hulls combustion at different values of EA. It is observed that the NOx emissions increase slightly with increasing EA. The variation of NOx emissions with SAR is described in figure 9b. It is noted that increasing SAR to 50% reduces NOx emissions from 350 ppm to 150 ppm (i.e. the reduction is about 45%).

The effect of using crushed bean hulls on NOx emissions is shown in Fig. 10a. It can be noticed that the NOx emissions decrease with decreasing EA and it reaches a minimum value of 140 ppm at EA =1.1. Generally, the NOx emissions have lower values (140-210 ppm) compared with that in case of using uncrushed bean hulls (350-430 ppm). Figure 10b shows the NOx emissions (without relating to 7% O2 in flue gas) from crushed bean hulls combustion along the CFB reactor at EA =1.4 and SAR = 0%. The NOx emissions increase with increasing the height above distributor till z=0.8 m and then asymptote to almost a constant value of 140 ppm.

The comparison of CO and NOx emissions from bean hulls combustion before and after the crushing indicates that the crushing reduces these emissions.

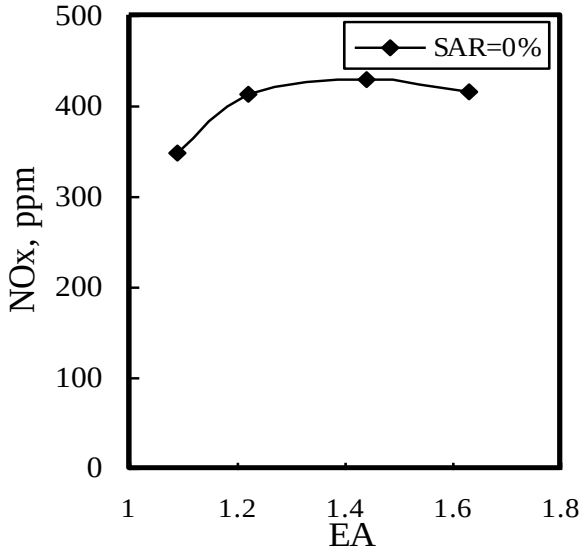

(a)

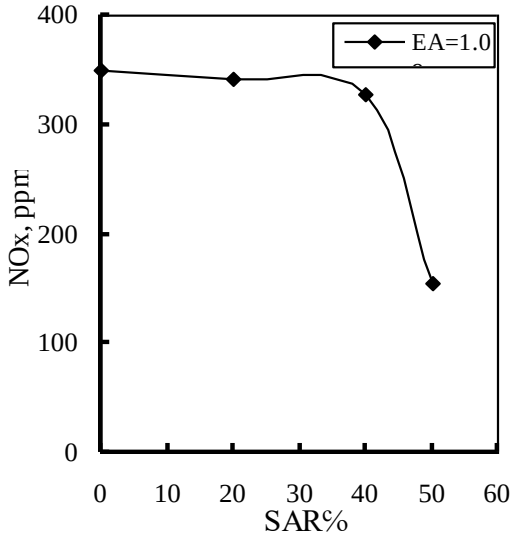

(b)

Figure 9: NOx emission for bean hulls combustion (a) at different EA. (b) at different SAR.

A.4 Combustion efficiency

The combustion efficiency is indicated in Table 4. In general, high combustion efficiency is mainly attributed to the reduction in unburned fixed carbon and low CO emissions within flue gas. The highest efficiency (98.5%) was achieved from the combustion of bean hulls at EA=1.09. The effect of SAR on the combustion efficiency is shown in Fig. 11. It can be observed that, increasing SAR causes a decrease in the combustion efficiency

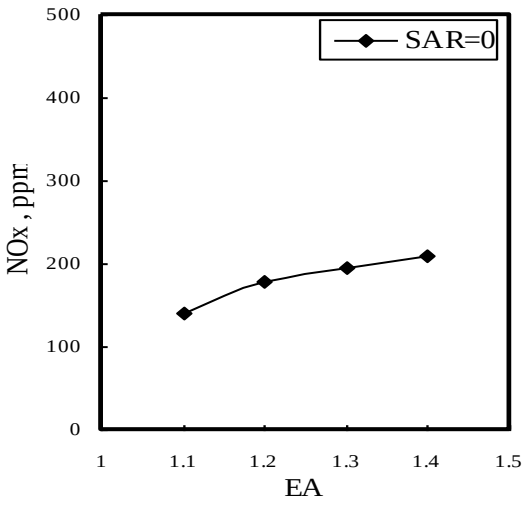

(a)

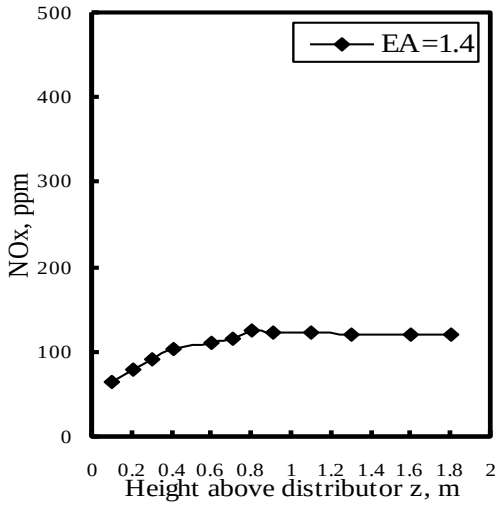

(b)

Figure 10: NOx emission for crushed bean hulls (a) at different EA. (b) along the reactor.

Table 4: The combustion efficiency of bean hulls

EA	SAR%	char%	$\eta_{c\%}$	EA	SAR%	char%	$\eta_{c\%}$
1.09	0	1.75	98.5	1.44	0	0.875	98.3
	20	2.7	98.2		20	1.5	98.1
	40	3.1	98		40	3.6	97.2
	50	3.4	97.7		50	3.9	96.6

Figure 11: Combustion efficiency for bean hulls combustion.

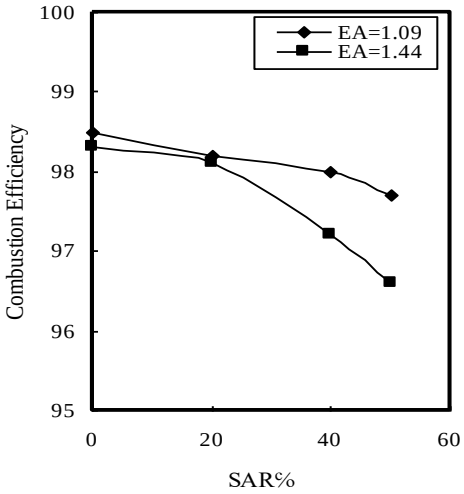

Figure 11: Combustion efficiency for bean hulls combustion.

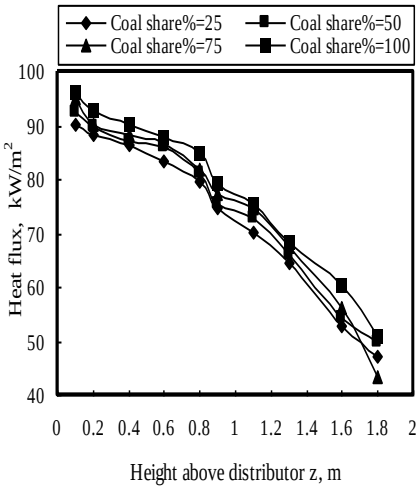

Figure 13: Heat flux for co-combustion of bean hulls and Sinai coal.

B. Co-combustion of bean hulls and Sinai coal

B.1 Temperature distribution

The temperature profiles for the co-combustion of crushed bean hulls mixed with Sinai coal are plotted in Fig. 12. The temperature was measured at EA= 1.09 and coal share of 25 %, 50 %, 75 % and 100 % of the thermal load. It is noticed that the temperature levels increase with increasing the coal share percentage. The maximum value of temperature (970^{o}C) is achieved at coal share of 100%.

B.2 Heat flux

Figure 13 shows the heat flux along the reactor height. It is clear that the heat flux has a similar trend of the temperature distribution (Fig. 12). The heat flux values increase with increasing the coal share. This may be attributed to the much elutriated burned char along the reactor during coal combustion where the fixed carbon content in coal is more than two times that in bean hulls. The maximum value of heat flux (96.25 kW/m^2) is at coal share of 100 %.

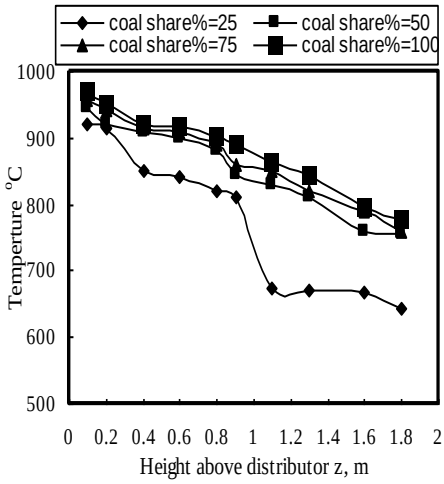

Figure 12: Temperature distribution for Co-combustion of bean hulls and Sinai coal.

B.3 Gas emission

The CO emissions variation with coal share percentage is shown in Fig. 14a. The CO emissions decrease with increasing the coal share percentage. This may be attributed to the higher density of coal particles comparing with biomass particles. Hence, the most char formed, after the volatiles leave the coal particle, may stay in the bed until burn completely. On the other side, the lower density of been hulls causes elutriation of particles without complete burning due to the short residence time of particles. In the same time, the separation efficiency of the cyclone may be insufficient to capture the elutriated bean hulls particles due to their low densities.

The effect of excess air ratio on CO emissions from co-combustion is shown in Fig. 14b. It is notable that the CO emissions increase with increasing EA for 25%, 50% and 75% coal share. This may be referred to the insufficient residence time for burning fuel particles completely with increasing fluidizing velocity. Another reason may be the lower temperature resulted from increasing excess air. It is also noticed that EA has no large effect on CO emission when coal share is 100%.

Figure 15a shows the variation of NOx emissions with coal share, the NOx emissions decrease as coal share increases. It is worth to note that this trend of NOx acts the same manner of CO emissions trend as shown previously in figure 14a. The NOx emissions exhibits low values lie between 10 ppm and 95 ppm. The effect of EA (1-1.8) which changes the fluidizing velocity, from1.15 m/s to 1.8 m/s, on NOx emissions is shown in Fig. 15b. The NOx emissions decrease as the excess air ratio increases. This may be explained with the cooling effect of much EA. The NOx emissions are in a low range of 8–95 ppm.

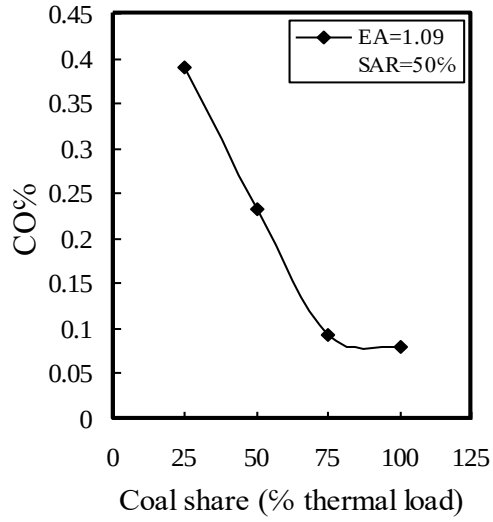

(a)

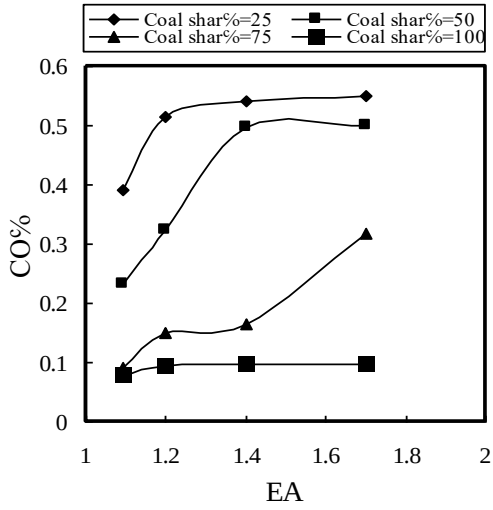

(b)

Figure 14: CO emissions for co-combustion of crushed bean hulls and Sinai coal.

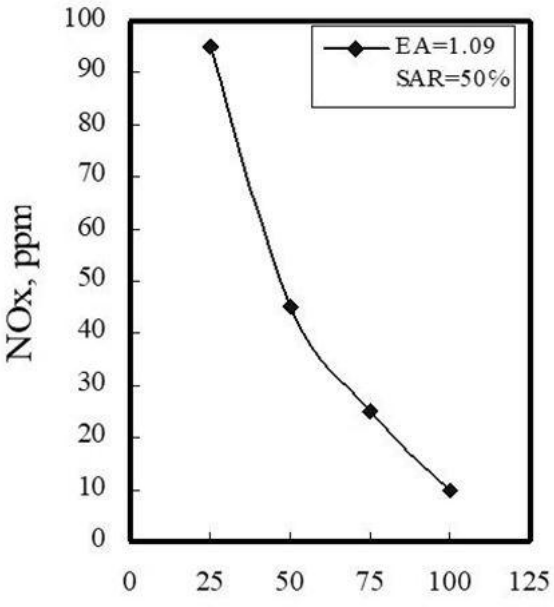

(a)

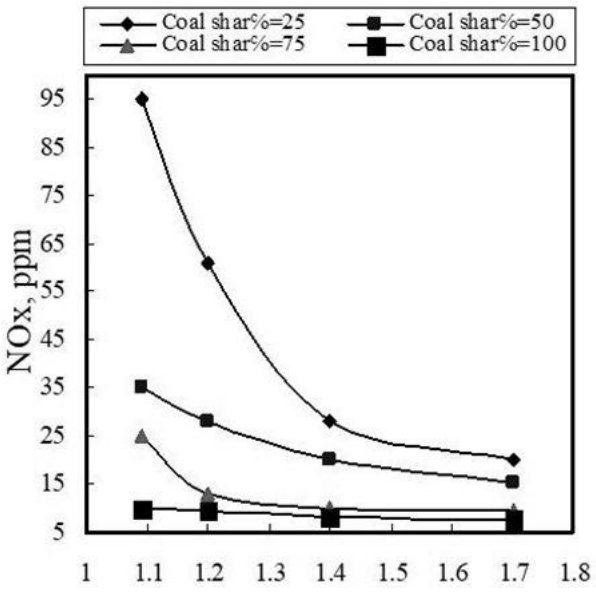

(b)

Figure15: NO_x emissions for co-combustion of crushed bean hulls and Sinai coal

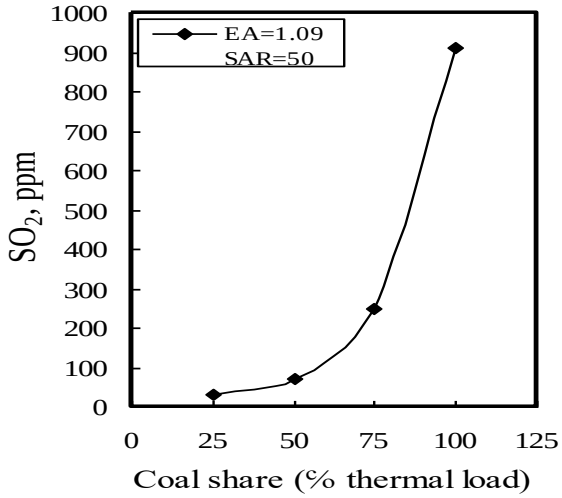

(a) at different coal share

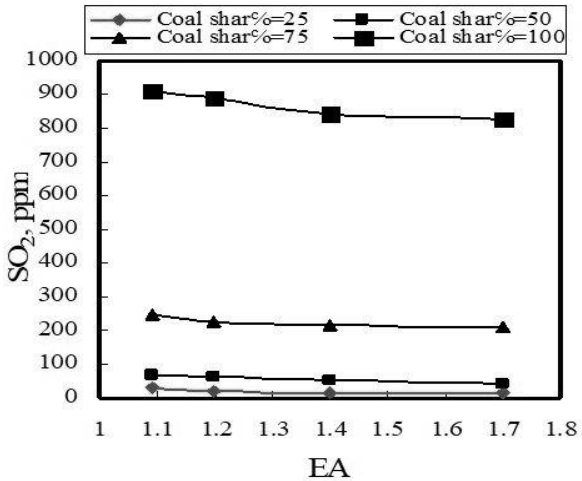

(b) at different EA

Figure 16: SO_2 emissions for co-combustion of crushed bean hulls and Sinai coal

IV. CONCLUSION

For the combustion of bean hulls, the temperatures decrease with increasing EA. The highest bed temperature is in the range between 900 ^{o}C and 1000 ^{o}C. The heat flux has a similar trend to the temperature distribution along the reactor. Decreasing secondary air admission, at the combustion of bean hulls, decreases the CO emissions and increases the NOx emissions and the combustion efficiency. The highest efficiency (98.5%) is achieved from the combustion of bean hulls at EA=1.09. The size reduction of bean hulls offers lower CO and NOx emissions from combustion.

For the co-combustion of bean hulls and Sinai coal, The temperatures and heat flux increase with increasing the coal share. The CO and NOx emissions decrease as the coal share increases. The CO emissions increase and NOx decrease with increasing EA for 25%, 50% and 75% coal share. The NOx emissions exhibits low values lie between 10 ppm and 95 ppm. The SO_2 emissions increase with increasing the coal share which provides more sulfur content in the fuel mixture. The values of SO_2 emissions varied between 30 ppm to 910 ppm.

REFERENCES

1. J Han, H Kim, W Minami, T Shimizu, G Wang, “The effect of the particle size of alumina sand on the combustion and emission behavior of cedar pellets in a fluidized bed combustor”, Bioresource Technology, vol. 99, 2008, pp. 3782–3786
2. M. Fang, L.Yang, G. Chen, Z. Shi, Z. Luo, K. Cen, "Experimental study on rice husk combustion in a circulating fluidized bed", Fuel Processing Technology, vol. 85, 2004, pp. 1273– 1282
3. F. Okasha, “Staged combustion of rice straw in a fluidized bed”, Experimental Thermal and Fluid Science, vol. 32, 2007, pp. 52-59
4. Z. Sun, B. Jin, M. Zhang, R. Liu, and Y. Zhang, "Experimental study on cotton stalk combustion in a circulating fluidized bed", Applied Energy, vol. 8, 2008, pp. 1027–1040
5. C. Serrano, H. Portero, E. Monedero, “Pine chips combustion in a 50 kW domestic biomass boiler”, Fuel, vol. 111, 2013, pp. 564–573
6. F. Miccio, A. Murri, V. Medri, E. Landi, “Agglomeration phenomena During Fluidized Bed Combustion/Gasification of Biomass Fuels”, CHEMICAL ENGINEERING TRANSACTIONS, vol. 74, 2019
7. F. Miccio, G. Ruoppolo, S. Russo, M. Urciuolo, A. Riccardis, “Fluidized Bed Combustion of Wet Biomass Fuel (Olive Husks)”, CHEMICAL ENGINEERING TRANSACTIONS, vol. 37, 2014
8. M. Youssef, "A comparative study for the combustion of Egyptian biomass in stationary and circulating fluidized bed", Minia journal vol. 28, 2009, pp.125-136
9. W. Permchart, and V. Kouprianov, "Emission performance and combustion efficiency of a conical fluidized-bed combustor firing various biomass fuels", Bioresource Technology vol. 92, 2004, pp. 83–92
10. J. Werther, M. Saenger, E. Hartge, T. Ogada, Z. Siagi, “Combustion of agricultural residues”, Progress in Energy and Combustion Science vol. 26, 2000, pp. 1-27
11. F. Miccio, R. Solimene, M. Urciuolo, P. Brachi, M. Miccio, “Fluidized bed combustion of a lignin-based Slurry”, Chem. Eng. Trans, vol. 50, 2016, pp. 271-276
12. E. Ferrer, M. Aho, J. Silvennoinen and R. Nurminen, "Fluidized bed combustion of refuse-derived fuel in presence of protective coal ash", Journal of Fuel Processing Technology, vol. 87, 2005, pp. 33-44
13. X. Jian-jun'y, Y. Xue-min, Z. D. Tong-li, S. Wen-li, and L. Wei-gang, "Emissions of SO2, NO and N20 in a circulating fluidized bed combustor during co-firing coal and biomass", Journal of Environmental Sciences, vol. 19, 2007, pp. 109-117
14. M. Youssef, S. Wahid, M. Wahhab, “ Combustion characteristics of Sinai coal and biomass in a circulating fluidized bed”, Proceeding of 32nd power plants technology conference, Dresden, Germany, 2000, pp. 41-51
15. M. Youssef, S. Wahid, M. Wahhab, A. Askalany, “ Experimental study on Egyptian biomass combustion in circulating fluidized bed”. Applied Energy vol. 86, 2009, pp. 2644-2650

AUTHORS PROFILE

Mahmoud Youssef is an Associate Professor at Jouf University, KSA. He received his Ph.D. in Mechanical Engineering from Minia University, Egypt in 1997. The PhD period included 2 years in TU Dresden, Germany for the experimental part from 1994 to 1996. He studied at Minia University, where he received his B.Sc. and M.Sc. degrees in Mechanical Power Engineering in 1986 and 1991, respectively. He was a teaching assistant, assistant professor and associate professor, in Mech. Eng. Dept, Minia University, in 1991, 1997 and 2013 respectively. His research interests include Combustion, Fuel, Energy utilization of biomass and heat and mass transfer.